18TH WORLD CONFERENCE ON EARTHQUAKE ENGINEERING
WCEE2024
MILAN

MILAN, ITALY
30TH JUNE - 5TH JULY 2024

www.wcee2024.it

EVALUATING DAMPING EFFECTS OF SEMI-ACTIVE CONTROL OF A BASE-ISOLATION SYSTEM UNDER NEAR-FAULT PULSE GROUND MOTIONS

H. Fujtani[1], M. Hashimoto[2], K. Nabeshima[2], Y. Mukai[2] & E. Sato[3]

[1] Kobe University, Kobe City, Japan, fujitani@kobe-u.ac.jp

[2] Kobe University, Kobe City, Japan

[3] National Research Institute for Earth Science and Disaster Resilience, Miki City, Japan

Abstract: *For a base-isolation system, controlling the response using semi-active dampers is effective at reducing the base-isolation layer's response displacement without increasing the superstructure's floor accelerations. Consequently, the building functions can be maintained. Usually, the damping effect is evaluated according to the maximum values of the base-isolation layer's response displacements and the superstructure's floor accelerations. However, structural engineers can benefit from a better understanding of the control effect using a simple physical value, such as the damping factor, when selecting the control algorithm. Trials to evaluate the control effects using a simple physical value are under development, although a few examples can demonstrate the control effect by the damping factor in cases of passive control systems. This study was conducted to formulate procedures providing a physical value to evaluate the damping effect of the control algorithm for a semi-active control method. Damping effects found from large-scale shaking table tests of a base-isolation system using various control algorithms were evaluated using a system identification method. This shaking table test was conducted at E-Defense of the National Research Institute for Earth Science and Disaster Resilience (NIED), which verified the damping effects under the Sylmar 1994 NS and Takatori 1995 NS ground motions using control methods proposed by researchers of five institutes of Japan and the US. The time history of acceleration of ground motions and the superstructure's floor accelerations were used for calculating the damping factors for some control algorithms. Evaluating the damping effect was possible according to the value of the damping factor. However, calculating the damping factor adequately was challenging in a few cases that adopted the control algorithm to generate a comparably larger or nonlinear damping force to piston velocity. This point will be explored further in future studies.*

1. Introduction

When a base-isolation system is excited by large earthquake ground motion, such as near-fault pulse ground motion generated during an intraplate earthquake, the deformation of the base-isolation layer exceeds the clearance, causing the structure to collide with a retaining wall, for example, as described by Hall et al. (1995). Therefore, reducing the response displacement of the base-isolation layer is necessary. However, attempts to reduce the response displacement by increasing the number of conventional passive dampers will increase the acceleration of the superstructure, thereby compromising the benefits of the base-isolation system. Semi-active control, which can vary damping characteristics, is regarded as an effective countermeasure, as described by, for example, Johnson et al. (1998) and Fujitani et al. (2003). As one semi-active control device, a magnetorheological fluid damper (MR damper) has been adopted for this study, as explained in earlier

reports by Rabinow (1948), Spencer et al. (1997), Sodeyama et al. (2003), among others. Magnetorheological fluids have yield stress which can be varied by application of a magnetic field. They have been attracting attention in recent years because they can obtain a large damping force with small amounts of electric power.

A large-scale shaking table test was conducted in 2019 at E-Defense, National Research Institute for Earth Science and Disaster Resilience (NIED), to verify the damping effect by semi-active control of the base-isolation system. For this experiment, researchers from Japanese and U.S. institutes proposed their original control methods using an MR damper and verified its effectiveness (Fujitani et al., 2020). The effectiveness of response reduction was organized by response values such as absolute acceleration of the superstructure and relative displacement of the base-isolation layer. However, if the response reduction effect of each control algorithm can be demonstrated using a physical quantity that can be recognized easily in common, such as the damping factor, then it is expected to provide an index for selecting a control method at the beginning of the design.

System identification is one effective method for understanding vibration characteristics such as damping factors and natural frequencies of buildings. Also, the Auto-Regressive with eXogenenous (ARX) model is a method for time-domain data (Saito, 1998). Based on this background, the purpose of this study is to evaluate the control effects in terms of damping factors using the ARX model based on results of a large-scale shaking table test on a semi-actively controlled base-isolation system conducted at E-Defense.

2. Outline of the E-Defense test

2.1. Test specimen

Figure 1 shows an overview of the test specimen. Figures 2 and 3 present elevation views of the test specimen. The test specimen, which is placed on the shaking table, is constrained in the orthogonal direction by a linear roller bearing. It is excited in the X-axis direction. Three input ground motions were used: El Centro 1940 NS 150%, Sylmar 1994 NS 50%, and JR Takatori 1995 NS 40% (Nakamura et al., 1996), (hereinafter designated as El Centro excitation, Sylmar excitation, and JR Takatori excitation). The mass of the superstructure was 14.9 tons as measured using a load cell. The stiffness of the laminate rubber bearing was calculated from the displacement-restoring force relation without electric current applied during the El Centro, Sylmar, and JR Takatori excitations. It was averaged at 44.9 kN/m for each value. Since the stiffness of the superstructure is much greater than that of the base-isolation layer, the test specimen can be regarded as a single-degree-of-freedom system (Sato et al., 2020). The natural period is 3.61 s. The natural frequency is 0.277 Hz. The damping factor of the laminate rubber bearing was identified as 3.58% based on the results of sinusoidal excitation tests.

Figure 1. Test specimen

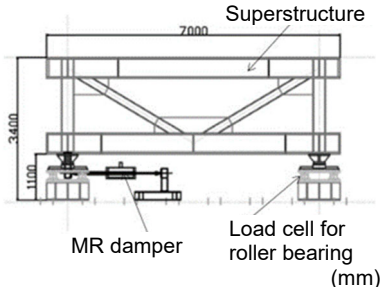

Figure 2. Schematic drawing of test specimen (X direction)

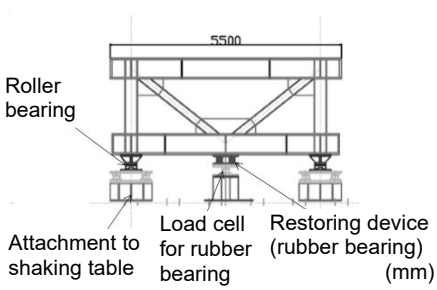

Figure 3. Schematic drawing of test specimen (Y direction)

2.2. MR damper

An MR damper uses a magnetorheological fluid (MR fluid), the yield stress of which changes depending on the magnetic field action inside the damper based on the mechanism of a conventional hydraulic damper. Figure 4 depicts a schematic diagram of the MR damper, in which magnetic particles are mixed in the base oil. When a magnetic field is applied, the magnetic particles form chains and clusters, which generate a resistive force in the direction perpendicular to the magnetic field when an oil flow is generated. The magnitude of the resistive force depends on the magnetic field strength, which varies with the value of the applied current,

making it possible to generate an arbitrary damping force. Figure 5 shows the relation between the shear rate and stress of an MR fluid. When a magnetic field is applied, a specific yield stress is generated, after which the viscous resistance increases in proportion to the shear rate, exhibiting the characteristics of a Bingham fluid. The damper force is modeled as shown in Equation (1), based on the single excitation experiment of the MR damper (Itahara et al., 2020).

$$F_{MR} = (-0.2261I^2 + 2.867I - 0.203)sign(v) + 2.11v \quad (1)$$

F_{MR} : *damper force* (kN) I : *applied electric current* (A) v : *damper piston velocity* (m/s)

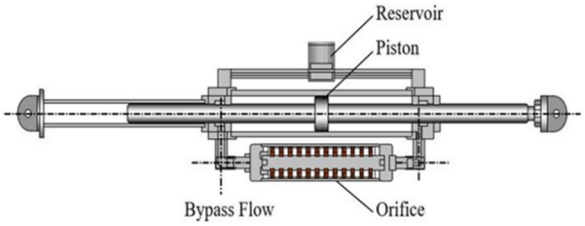

Figure 4. Schematic diagram of MR damper

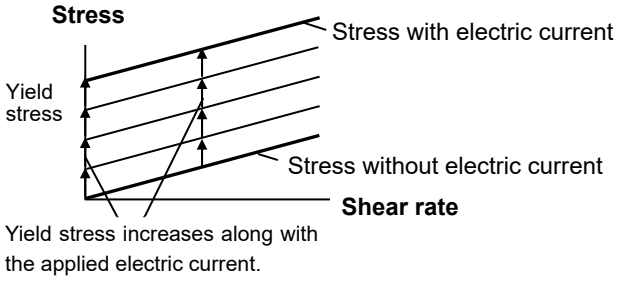

Figure 5. Relation between shear rate and yield stress

3. Control methods

The following seven control methods are examined among the 31 control methods verified in the E-Defense experiment.

Figure 6 shows the relation between the piston velocity and damper force of the MR damper under El Centro excitation for the following seven control methods.

1. Passive off

No current is ever applied regardless of the response.

2. Velocity-proportional control

Velocity-proportional control is a control method that simulates viscous damping, in which a damping force of a specific rate is applied to the damper in proportion to the piston velocity of the damper.

3. Variable damping coefficient (Kishida et al., 2020)

A control method that simulates a variable hydraulic damper enables switching of the damping coefficient to two levels: 10% and 30% (c_L=4.79 kN·s/m, c_H=14.37 kN·s/m) of the damping factor calculated from mass and stiffness of the test specimen. The target control force is obtained from the optimal regulator theory. The damping coefficient is set to c_H when the damper damping force is less than the target control force and to c_L when the damper damping force is greater than the target control force.

4. State feedback optimal control (Itahara et al., 2020)

State feedback optimal control is a control method that determines the control force to minimize the evaluation function using the magnitude of the response of the control target and the magnitude of the control force shown in Equation (2). The weight coefficients (α_a, α_v, α_d) of the control terms are set to El Centro excitation (α_a, α_v, α_d) = (10^8, 10^8, 10^8), Sylmar excitation (α_a, α_v, α_d) = (10^7, 10^7, 10^7), and JR Takatori excitation (α_a, α_v, α_d) = (10^7, 10^7, 10^7). Here, $x(t)$, $\dot{x}(t)$, and $\ddot{x}(t)$ respectively denote the response displacement, response velocity and response acceleration of the superstructure. Also, $\ddot{z}$ and $f(t)$ respectively represent the acceleration of ground motion and control force.

$$J = \int_0^\infty (\alpha_d x(t)^2 + \alpha_v \dot{x}(t)^2 + \alpha_a (\ddot{x}(t) + \ddot{z})^2 + \gamma f(t)^2) dt \quad (2)$$

α_d : w*eight coefficient for relative displacement* α_v : w*eight coefficient for relative velocity*

α_a : w*eight coefficient for absolute acceleration* γ : w*eight coefficient for control force*

5. State feedback energy function control (EF control) (Itahara et al., 2020)

EF control is a control method that uses the sum of kinetic energy and elastic strain energy as the evaluation function, as shown in Equation (3). It causes the MR damper to output a small hysteresis loop for small ground motions and a large hysteresis loop for large ground motions. The values of λ are λ = 175 for El Centro excitations, λ = 125 for Sylmar excitations, and λ = 50 for JR Takatori excitations.

$$F = \lambda\sqrt{\frac{1}{2}m\dot{x}^2 + \frac{1}{2}kx^2} \quad \lambda : \text{w}\textit{eight coefficient} \tag{3}$$

6. Eventual sliding mode control (Ito et al., 2020)

Eventual sliding mode control is a control method by which the system state reaches sliding mode at the final switching plane without reaching sliding mode at other switching planes. As shown in Equation (4), the control force consists of a linear state feedback control term and a nonlinear control term.

$$u = u_l + u_{nl} = -(SB)^{-1}SAx - \eta\frac{\sigma}{\|\sigma\|} \qquad \eta : \textit{switching gain of nonlinear inputs} = 4000 \tag{4}$$

7. Modulated homogeneous friction control (Christenson et al., 2020)

Variable friction control is a control method by which the current applied to the damper is the maximum relative displacement multiplied by a constant, as shown in Equation (5).

$$i_{cmd}(t) = g \times |P[x_{rel}(t)]| \tag{5}$$

i_{cmd} : command electric current (A)

g : positive gain, based on a maximum applied current for a set relative displacement (g =45)

$x_{rel}(t)$: *damper relative displacement* P : *prior-local-peak (or prior-to-peak) operator*

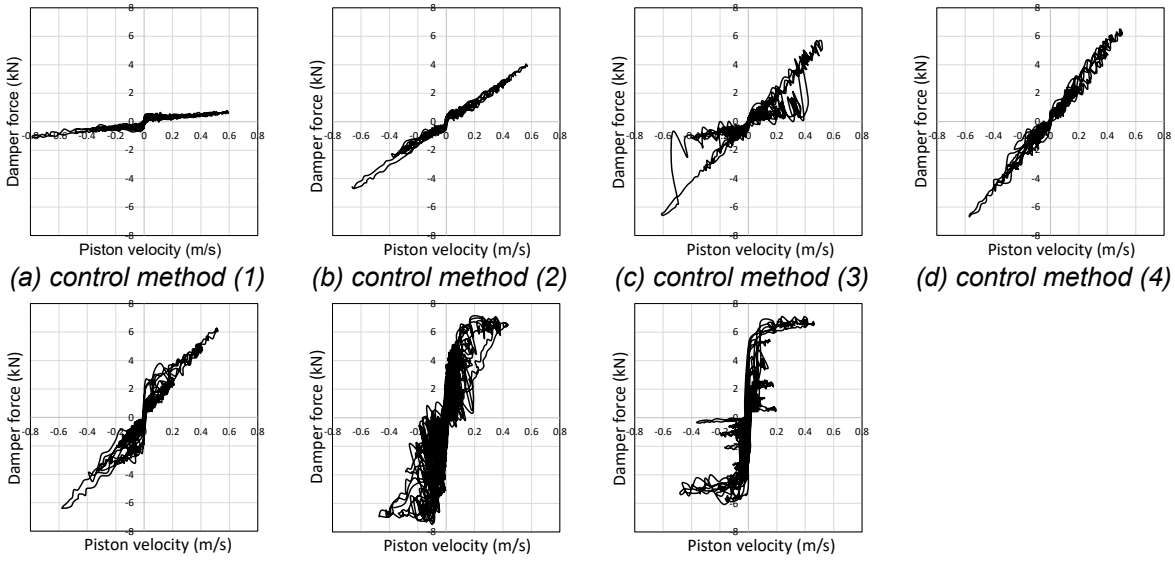

(a) control method (1) *(b) control method (2)* *(c) control method (3)* *(d) control method (4)*

(e) control method (5) *(f) control method (6)* *(g) control method (7)*

Figure 6. Relation between piston velocity and damping force of MR damper

4. Identification method for damping factor

4.1. Auto-Regressive with eXogenous (ARX) model

The ARX model is described as a digital filter acting on input and output signals. It is a transfer function type model where the coefficients of the filter are unknown parameters. The ARX model, proposed for one-input, one-output identification, has been extended to multi-input, multi-output problems (Saito, 1998). The ARX model generally assumes that the building behaves linearly. Still, the test specimen used for this study has a roller bearing that generates highly nonlinear friction forces, as shown in Figure 7(a). Therefore, the friction force of the roller bearing was calculated by subtracting the restoring force of the rubber bearing and the damping force of the MR damper from the inertial force of the mass, as shown in Figure 7(b).

In this study, the closed-loop direct identification method (Ljung, 1999, Ikeda, 2004) is applied to identify the model with the observed ground motions (Figure 8(a)), and accelerations derived from the calculated friction force divided by mass (Figure 8(b)) as inputs and the response of the control object as output, and the two-input, one-output ARX model is applied. The ARX model is expressed as in Equation (6), where $A(q)$ and $B(q)$ are polynomials of the time delay operator q^{-j} expressed in Equation (7), and where $e(t)$ is white noise. The natural frequencies and damping factors are calculated from the roots ${}_zp_j$ of the polynomial $A(q)$ using Equation (8). Additional meanings of the symbols in Equations (7) and (8) are presented by Saito (1998).

The analysis time range is 35 s. The identification results are averaged over ten durations with analysis start times of 1, 2, ..., and 10 s. To reduce the effort necessary to determine the model order before identification, a bandpass or low-pass filter was applied to adjust the transmission frequency range of 0.0-1.5 Hz to include the peak frequency of the transfer function. Furthermore, acceleration data sampled at 100 Hz are converted to 10 Hz and are used for analyses by reducing the sampling frequency.

Time history response analysis is conducted on a single-degree-of-freedom system simulating the test specimen. The results are used to verify the accuracy of the identification using the two-input, one-output ARX model used for this study. The stiffness and mass of the model are the values presented in Chapter 2. The damping factor is set as 0.2. One input is the acceleration recorded on the shaking table; the other is the friction force measured in the El Centro excitation test without an electric current applied. Figure 8 shows the shaking table acceleration, the acceleration obtained from the frictional force divided by mass, and the absolute acceleration of the superstructure obtained from the time history response analysis. Figure 9 presents the results of identifying the damping factors and natural frequencies. Bandpass filters of two types were used for this analysis: 0.1–0.5 Hz and 0.1–0.4 Hz. As the figure shows, the natural frequencies and damping factors can be identified accurately using the two-input, one-output ARX model.

$$A(q)y(t) = B(q)u(t) + e(t) \tag{6}$$

$$A(q) = 1 + \sum_{j=1}^{na} a_j q^{-j}, \qquad B(q) = \left[\sum_{j=1}^{mn n_b} {}_{mn}b_j q^{-j+1-mn n_k}\right] \tag{7}$$

$$f = \frac{\left|log_e\ {}_zp_j\right|}{2\pi\Delta t}, \qquad h_{ARX} = \frac{-log_e\left|\ {}_zp_j\right|}{2\pi f\,\Delta t} \tag{8}$$

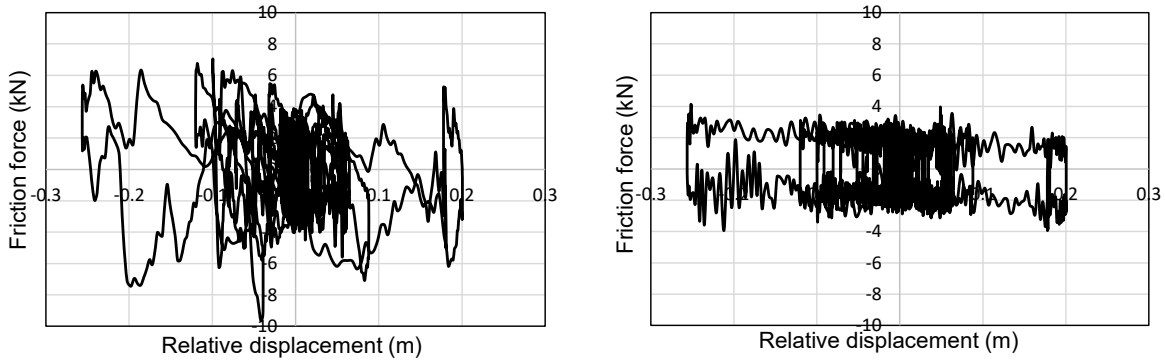

(a) Measured friction force *(b) Calculated friction force*

Figure 7. Relation between relative displacement and friction force of roller bearing

(El Centro excitation input, passive off)

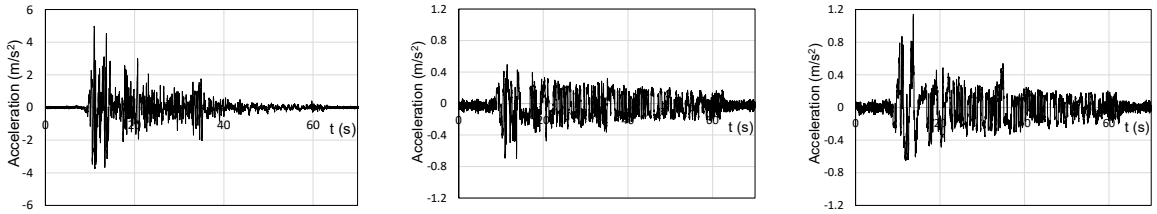

(a) Acceleration of shaking table *(b) Acceleration derived from calculated friction force divided by mass* *(c) Absolute acceleration of superstructure*

Figure 8. Time history of acceleration

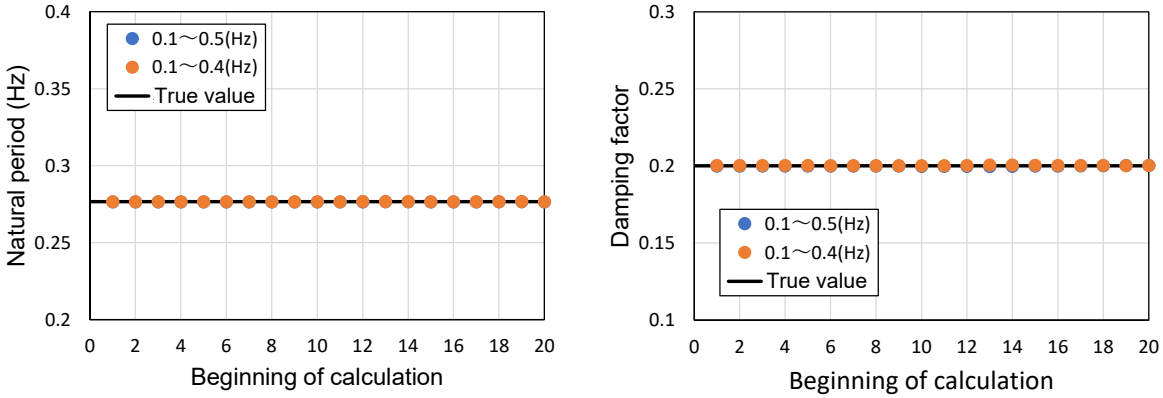

(a) Natural frequency *(b) Damping factor*

Figure 9. Identification results obtained using the two-input one-output ARX model

4.2. Approximate damping factor

To compare the results of the identification with the ARX model, the damping factor h_{MR} of the damper is obtained from the damping coefficient as a proportional constant decided from a linear approximation of the piston velocity - damper force relation of the damper in the test data. It is added to the damping factor h_s of the structure, as shown in Equation (8), to obtain an approximate damping factor h.

$$h = h_{MR} + h_s \tag{8}$$

5. Identification results

Figure 10 presents the damping factors identified using the methods described in Chapter 4. Table 1 shows the identification results of the natural frequencies by the ARX model, which were obtained when the differences between the identified natural frequencies and those of the test specimen were the smallest among the results obtained by application of several types of filters. Results show that, for control methods (2), (3), (4), and (5), where the damper force is regarded as behaving linearly (Figure 6), the approximate damping factors and the damping factors identified by the ARX model have similar values. In contrast, for control methods (6) and (7), where strong nonlinearities are observed (Figure 6), the identified values of the damping factors vary widely. The damping factors differ depending on the input earthquake ground motions, even for the same control method.

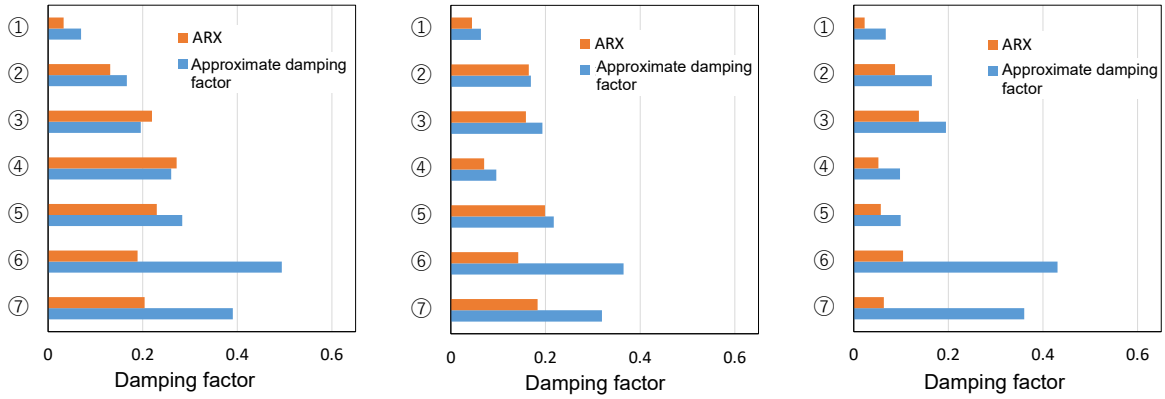

(a) El Centro excitation *(b) Sylmar excitation* *(c) JR Takatori excitation*

Figure 10. Identification results of damping factor by ARX model

Table 1. *Identification results of natural frequency by ARX model* (Hz)

Control method	El Centro excitation	Sylmar excitation	JR Takatori excitation
(1)	0.2763	0.2767	0.2794
(2)	0.2818	0.2789	0.2798
(3)	0.2608	0.2612	0.2703
(4)	0.2746	0.2821	0.2756
(5)	0.2769	0.2733	0.2776
(6)	0.2746	0.2724	0.2966
(7)	0.2767	0.2790	0.2730

* Control methods are described in Chapter 3 with the number

6. Discussion of the identified results

Figure 11 presents the relation between the damping factors identified by the ARX model and the experimentally obtained results. The experimentally obtained response values include the effect of friction force because of the linear roller bearing, but the damping factors identified are those because of the MR damper and the laminated rubber bearing by identifying with the two-input, one-output ARX model described in Chapter 4. Results show that, for all earthquake ground motions, except for (6) Eventual sliding mode control and (7) Modulated homogeneous friction control, the relation between the damping factors and the experimentally obtained results is generally as one might expect (relative displacement is reduced for larger damping factors and absolute acceleration is increased for larger damping factors). Strong nonlinearity of the damper force is regarded as affecting the ARX model identification results for the (6) Eventual sliding mode control and (7) Modulated homogeneous friction control, as shown in Figure 6.

In the case of El Centro excitation and Sylmar excitation, (3) Control simulating a variable hydraulic damper, (4) State feedback optimal control, and (5) EF control were shown to reduce displacement while maintaining the same level of acceleration compared to (1) Passive off. On the other hand, when JR Takatori excitation was input, none of the controls showed a significant response reduction effect on displacement. The absolute acceleration RMS values were amplified greatly by (6) Eventual sliding mode control and (7) Modulated homogeneous friction control compared to (1) Passive off, indicating that the semi-active control was less effective.

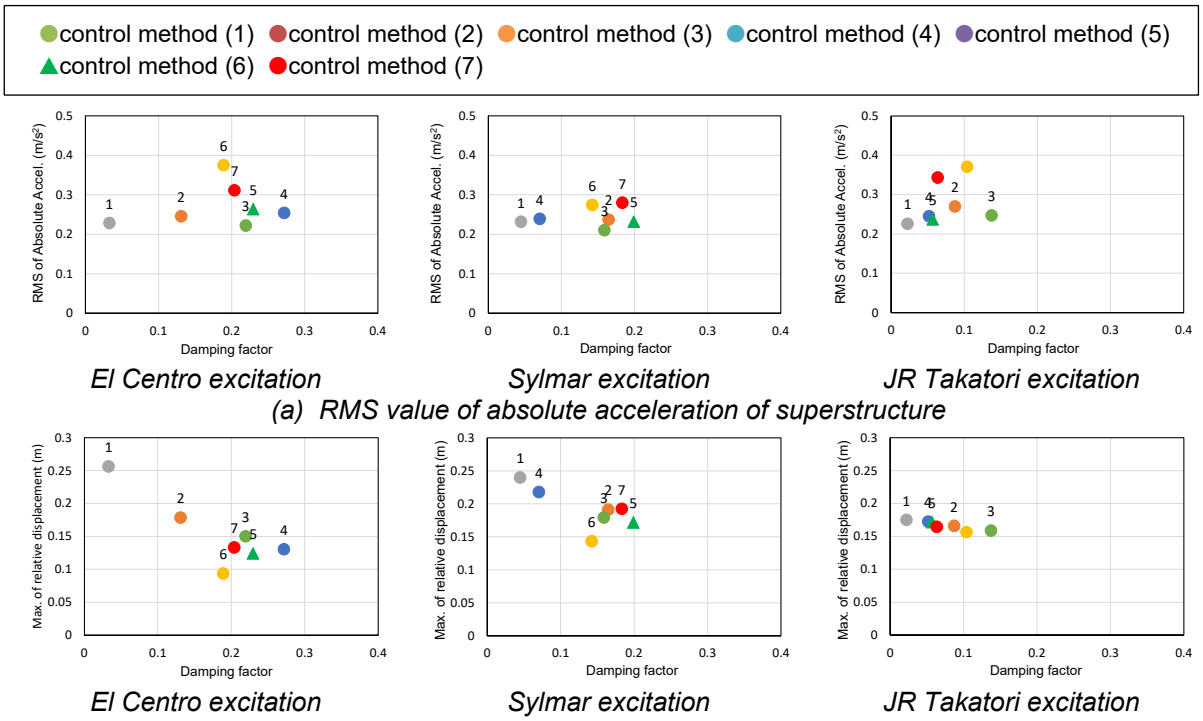

El Centro excitation *Sylmar excitation* *JR Takatori excitation*

(a) RMS value of absolute acceleration of superstructure

El Centro excitation *Sylmar excitation* *JR Takatori excitation*

(b) Maxim value of relative displacement of the base-isolation layer

Figure 11. Relation between damping factor identified by ARX model and test results (Acceleration and Displacement)

7. Verification by response analysis

The validity of the identification results was verified by comparing the analytical results with the experimentally obtained data from an analysis using the shaking table acceleration and friction force as inputs. Figure 12 presents the relation between calculated responses using the identified natural frequency and damping factor from the ARX model (Simulation by ARX model) and calculated responses using the acceleration of the shaking table and estimated friction force (Experiment simulation). Figure 13 presents the relation between calculated responses using the original natural frequency and approximate damping factor, as described in section 4.2 (Simulation by approximate model), and calculated responses using the acceleration of the shaking table and estimated friction force (Experiment simulation). Dashed lines in the figures represent errors of ±15% and ±20%. Here, the mass of the model is 14.9 tons.

As shown in Figure 12, the results of the ARX model identification are useful to predict the absolute acceleration RMS values within 15% error, except for control methods (6) and (7) for all input ground motions. The relative displacement of the base-isolation layer can be predicted within almost 15% error for any control method except (6) for Sylmar excitation and JR Takatori excitation.

As shown in Figure 13, the results obtained using the approximate damping factor are useful to predict the absolute acceleration RMS values within 15% error for all control methods for all input ground motions. The relative displacement of the base-isolation layer was predicted within almost 15% error for all control methods except (7) for all the input ground motions.

As presented in the discussion above, when the ARX method was used, the error sometimes exceeded 20% by a large margin. This was particularly the case for control methods (6) and (7), where a large damping force was exerted even when the piston velocity was small. Even in such cases, the error was generally less than 20% when approximate damping was used.

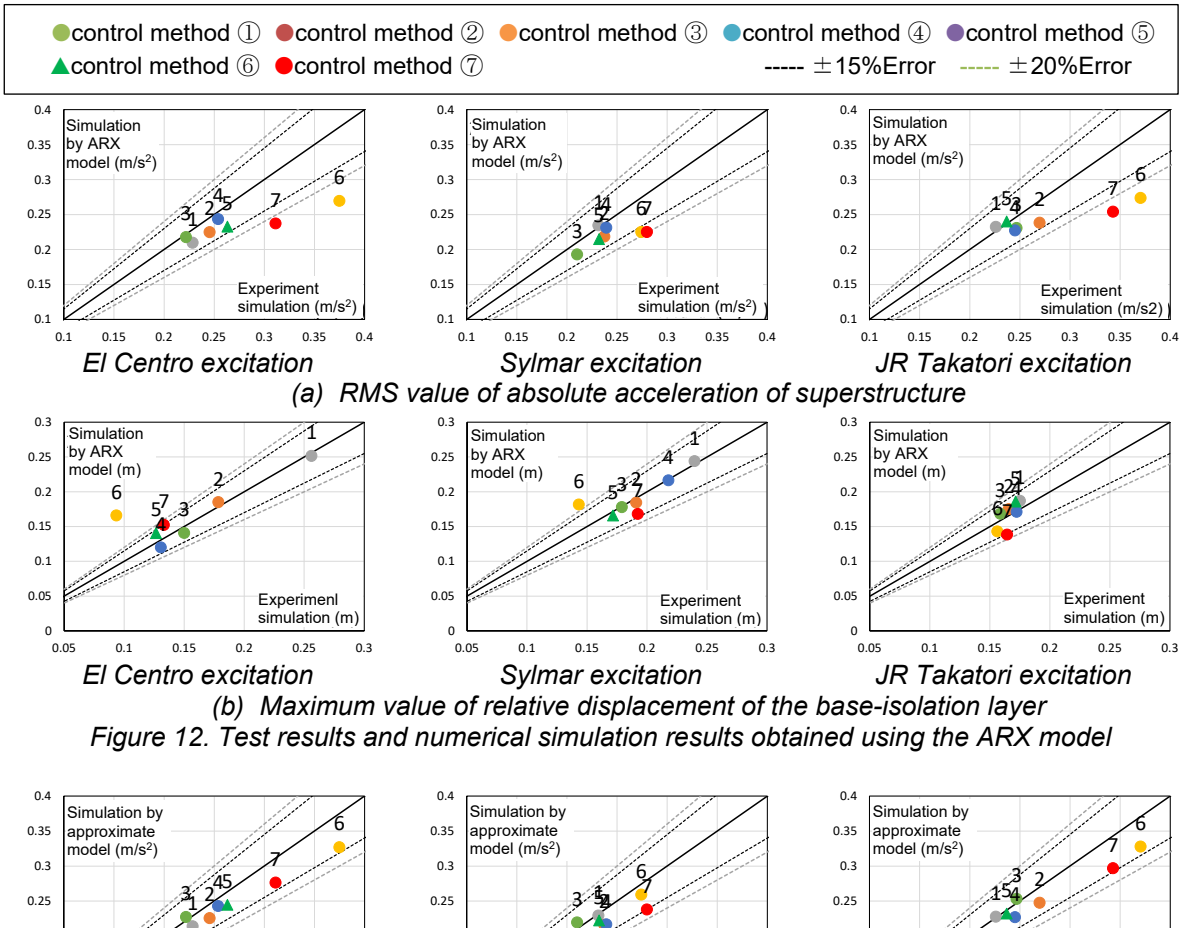

(a) RMS value of absolute acceleration of superstructure

(b) Maximum value of relative displacement of the base-isolation layer

Figure 12. Test results and numerical simulation results obtained using the ARX model

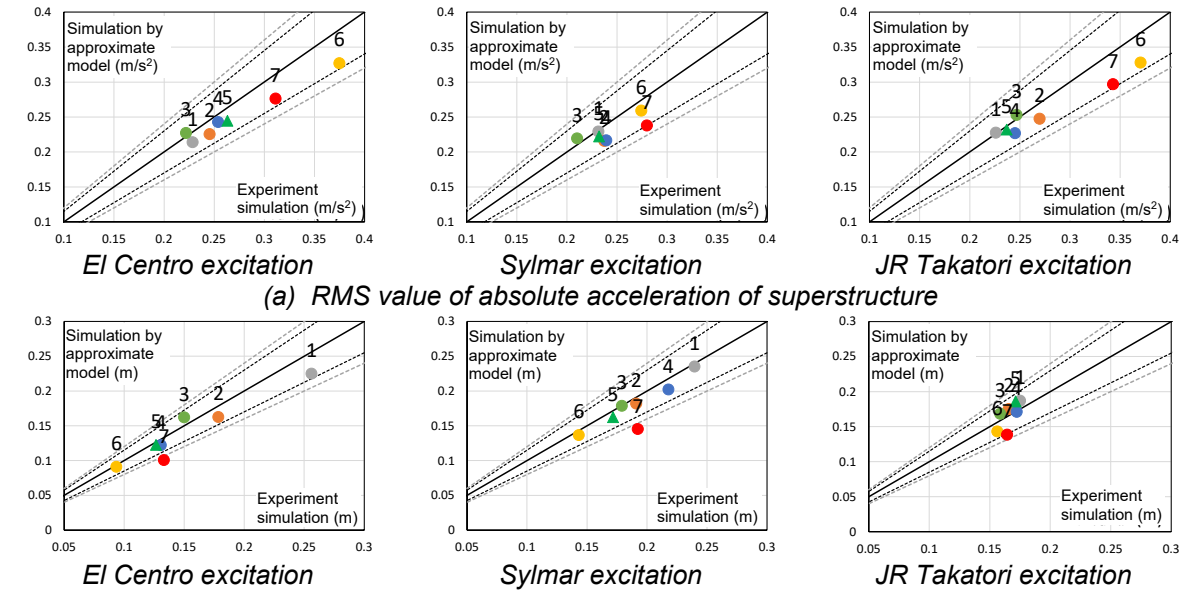

(a) RMS value of absolute acceleration of superstructure

(b) Maximum value of relative displacement of the base-isolation layer

Figure 13. Test results and numerical simulation results obtained by approximate damping

8. Conclusions

To evaluate the damping performance of semi-active control, the ARX model was applied to experimentally obtained data of a large-scale shaking table experiment conducted at E-Defense for semi-active control of the base-isolation system to estimate the damping factors for the respective control methods. To verify the validity of the results, a time history response analysis was performed by application of the identified values (damping factors and natural frequencies) to a single-degree-of-freedom system simulating the E-Defense test model. Results confirmed that the ARX model-estimated damping factors show the control effect qualitatively, except for the control method with strong nonlinearity, based on the relation between the ARX model-estimated damping factors and the experimentally obtained results. Time history response analysis using the damping

factors estimated using the ARX model was able to predict the absolute acceleration RMS values with good accuracy, except for the control method with strong nonlinearities.

Acknowledgment

This work was supported by JSPS KAKENHI Grant Number JP22H01643.

References

Christenson R., Stevens M., Sato E., Fujitani H., Mukai Y. (2020). PERFORMANCE OF SEMI-ACTIVE CONTROLLERS FOR A LARGER SCALE BASE-ISOLATION STRUCTURE WITH MR DAMPER *Proceedings of the 17th World Conference on Earthquake Engineering (17WCEE)*, Paper No. 2g-0253, Sendai, Japan.

Fujitani H., Shiozaki Y., Hiwatashi T., Soda S. (2003). Innovation of Low Frequency Buildings by Semi-Active Control by Using an MR Damper, *Proceedings of the CIB-CTBUH International Conference on Tall Buildings, CIB Publication No:290*, Kuala Lumpur, Malaysia: 551-558.

Fujitani H., Mukai Y., Sato E., Johnson E. A., Christenson R., Kishida A., Ito M., Shima T., Itahara K., Iba S., Honma A., Fukui H. (2020). Comparison of E-Defense Test Results by Five Institutes of Semi-Active Control of Base-isolation System, *Proceedings of the 17th World Conference on Earthquake Engineering (17WCEE)*, Paper No. 2g-0130, Sendai, Japan.

Hall J. F., Heaton T. H., Halling M. W., Wald D. J. (1995). Near-Source Ground Motion and its Effects on Flexible Buildings, *Earthquake Spectra*, Volume 11, No.4: 569-605.

Ikeda Y. (2004). Application of Direct Identification on Closed Loop to Earthquake Observations Record in Actively-Controlled Structures, *Journal of Structural and Construction Engineering*, Vol.69, No.581: 47-54. (in Japanese)

Itahara K., Fujitani H., Mukai Y., Ito M., Sato E., Iba S. (2020). SHAKING TABLE TEST AND REAL-TIME HYBRID SIMULATION IN SEMI-ACTIVE CONTROLLED BASE-ISOLATION SYSTEM, *Proceedings of the 17th World Conference on Earthquake Engineering (17WCEE)*, Paper No. 2g-0136, Sendai, Japan.

Ito M., Fujitani H., Mukai Y., Sato E., Kishida A., Itahara K., Iba S., Johnson E. A., Christenson R. (2020). EVENTUAL SLIDING MODE CONTROL FOR AN ISOLATED STRUCTURE USING MR DAMPER, *Proceedings of the 17th World Conference on Earthquake Engineering (17WCEE)*, Paper No. 2g-0109, Sendai, Japan.

Johnson E. A., Ramallo J. C., Spencer Jr. B. F., Sain, M. K. (1998). Intelligent Base Isolation Systems, *Proceedings of the Second World Conference on Structural Control*, Kyoto, Japan: 367–376.

Kishida A., Sato E., Iba S., Fujitani H., Mukai Y., Itahara K., Johnson E. A., Kajiwara K. (2020). Semi-active control of base-isolated structure using MR damper that simulates variable hydraulic damper and complex stiffness damper, *Proceedings of the 17th World Conference on Earthquake Engineering (17WCEE)*, Paper No. 2g-0134, Sendai, Japan.

Ljung L. (1999). System Identification: Theory for the User (2nd Edition), Prentice Hall PTR.

Nakamura Y., Uehan F., Inoue H., (1996). Waveform and its Analysis of the 1995 Hyogo-Ken-Nanbu Earthquake (II), *JR Earthquake Information* No. 23d, Railway Technical Research Institute. (in Japanese)

Rabinow J. (1948). The Magnetic Fluid Clutch, *AIEE Transactions*, Vol.67: 1308-1315.

Saito T. (1998). System Identification of a High-rise Building Applying Multi-Input-Multi-Output ARX Model of Modal Analysis, *Journal of Structural and Construction Engineering*, Vol.63, No.508: 47-54. (in Japanese)

Sato E., Kishida A., Kajiwara K., Fujitani H., Mukai Y., Ito M., Itahara K., Iba S., Johnson E. A., Christenson R. (2020)：OUTLINE OF E-DEFENSE SHAKING TABLE TESTS FOR SEMI-ACTIVE CONTROL OF BASE-ISOLATION SYSTEM, *Proceedings of the 17th World Conference on Earthquake Engineering (17WCEE)*, Paper No. 2g-0212, Sendai, Japan.

Sodeyama H., Sunakoda K., Fujitani H., Soda S., Iwata N., Hata K. (2003). Dynamic Tests and Simulation of Magneto-rheological Damper, *Computer-Aided Civil and Infrastructure Engineering*, Vol.18, Iusse 1: 45-57.

Spencer Jr. B. F., Dyke S. J., Sain M. K., Carlson J. D. (1997). PHENOMENOLOGICAL MODEL FOR MAGNETORHEOLOGICAL DAMPERS, *ASCE Journal of Engineering Mechanics*, 123(3): 230-238.